ORNL/TM-2022/2812

A Comparison of the Radiation Shielding Requirements of Select Radioisotopes for Potential Use in Radioisotope Power Systems

Noel Nelson
Brad Johnson

April 2023

OAK RIDGE National Laboratory

ORNL IS MANAGED BY UT-BATTELLE LLC FOR THE US DEPARTMENT OF ENERGY

ORNL/TM-2022/2812

Nuclear Energy and Fuel Cycle Division

A COMPARISON OF THE RADIATION SHIELDING REQUIREMENTS OF SELECT RADIOISOTOPES FOR POTENTIAL USE IN RADIOISOTOPE POWER SYSTEMS

Noel Nelson
Brad Johnson

April 2023

Prepared by
OAK RIDGE NATIONAL LABORATORY
Oak Ridge, TN 37831
managed by
UT-BATTELLE LLC
for the
US DEPARTMENT OF ENERGY
under contract DE-AC05-00OR22725

CONTENTS

LIST OF FIGURES

LIST OF TABLES

ABBREVIATIONS

ANSI	American National Standards Institute
CADIS	Consistent Adjoint Driven Importance Sampling
DOE	US Department of Energy
DU	depleted uranium
MAVRIC	Monaco with Automated Variance Reduction using Importance Calculations
MCNP	Monte Carlo N-Particle
MMRTG	Multi-Mission Radioisotope Thermoelectric Generator
ORNL	Oak Ridge National Laboratory
RPS	Radioisotope Power System
RPS-DET	Radioisotope Power System – Dose Estimation Tool
RTG	radioisotope thermoelectric generator
SF	spontaneous fission
SNAP	Systems for Nuclear Auxiliary Power

ABSTRACT

Supplies of ^{238}Pu, one of the most widely used radioisotope power system fuels, have steadily decreased since the end of the Cold War. This has prompted the recent investigation of several radioisotopes as alternative fuels. In this work, the radiation shielding requirements of seven candidate radioisotope power system (RPS) fuels with relatively high thermal heat generation from alpha and beta decay were compared to ^{238}Pu. The candidate radioisotope battery fuel isotopes include ^{241}Am, ^{90}Sr, ^{244}Cm, ^{227}Ac, ^{228}Ra, ^{228}Th, and ^{232}U. The amount of each fuel was standardized to 100 W_{Th}, and the SCALE suite of codes, ORIGEN and MAVRIC, were utilized to perform the radiation transport simulations for each type of penetrating ionizing radiation (i.e., gamma, neutron, bremsstrahlung) emitted to the surrounding environment. Several types of shielding were considered, including graphite, depleted uranium, and mixed metal and graphite composite shields. ^{241}Am, and ^{238}Pu required no shielding to reduce the dose below 100 mrem/hr on contact. Ac-227 and Sr-90 required an intermediate amount of shielding (approximately 8 kg and 40 kg, respectively) to reach the same dose threshold, and the other isotopes required a large amount of shielding (varying from 100-1000 kg of total mass). The isotopes that require heavy shielding (i.e., ^{244}Cm, ^{228}Ra, ^{228}Th, and ^{232}U) are recommended for applications where weight is less of a mission constraint.

1. INTRODUCTION

Radioisotope thermoelectric generators (RTGs) are a type of RPS that have been used for spacecraft, marine, and terrestrial applications since the early 1960s. The earliest RTGs were the odd-numbered Systems for Nuclear Auxiliary Power (SNAP) series (Anderson and Featherston 1960). Historically, "US RTGs have used plutonium-238 as the source of heat for space missions because of its long half-life (87.8 years) and its comparatively low level of radiation emission. . ." (Bennett et al. 1996). Modern RPSs such as the Multi-Mission Radioisotope Thermoelectric Generator (MMRTG) are no exception and continue to be powered by ^{238}Pu fuel (Lee and Bairstow 2015). Terrestrial and marine RTGs have used ^{90}Sr as the radioisotope for fuel, and Oak Ridge National Laboratory (ORNL) fabricated over 30 of these RTGs in the 1960s (Shor et al. 1971).

Since the end of the Cold War, supplies of ^{238}Pu have steadily declined along with the decline in nuclear weapons material production. Currently, production of 1.5 kg of ^{238}Pu is planned annually in the United States to maintain program needs for the National Aeronautics and Space Administration (NASA), but production capacity beyond that is not likely without increased production facilities. (American Nuclear Society 2021) The ^{90}Sr used in previous RTGs was obtained from the Hanford site as a by-product from its plutonium production mission. The remaining ^{90}Sr from the Hanford production mission is designated for disposal, and no new ^{90}Sr is being produced specifically for RPS fuels. Sr-90 is a common fission byproduct, so it could also be recycled from commercial spent nuclear fuel.

Interest in long-duration power supplies for space and marine applications has recently been renewed. RPSs are a logical power supply for these environments, and significant quantities of radioisotopes will be required to fuel them. The need for radioisotopes to fuel RPSs and the lack of an adequate supply of ^{238}Pu and ^{90}Sr has generated interest in investigating alternate radioisotope fuels (Dustin and Borrelli 2021). One such radioisotope is ^{241}Am, which is of interest not just domestically, but is also the selected isotope of the European Space Agency as a heat source for spaceflight RPS (Ambrosi et al. 2019, Dustin and Borrelli 2021).

Several factors impact the selection of a radioisotope for a RPS application. The total size, weight and power output of an RPS power supply dictate the types of missions it can support. Thus, attributes such as

specific power, radiation shielding requirements, solubility in water, melting temperature, SNM classification, etc. become important parameters that influence application decisions.

Eight radioisotopes with high activities were selected for this study: ^{238}Pu, ^{241}Am, ^{90}Sr, ^{244}Cm, ^{227}Ac, ^{228}Ra, ^{228}Th, and ^{232}U. All but ^{90}Sr are alpha emitters, but some have other radioactive emissions as a part of their decay chains. These isotopes and their subsequent decay products emit high amounts of other types of radiation such as bremsstrahlung, gamma, and neutron radiation. An example of the decay tree for ^{228}Th is shown in Figure 1.

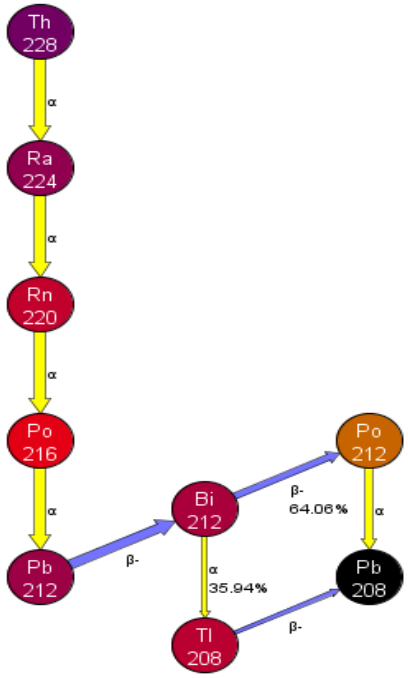

Figure 1. Th-228 decay chain from ENDF/B-VIII.0. (JANIS 2013)

Bremsstrahlung radiation is typically secondary x-ray emissions from beta radiation scattering in high-Z materials, and neutron radiation is typically caused by (α,n) reactions with oxygen, especially ^{18}O. Additionally, several of the eight isotopes may undergo spontaneous fission (SF), which also produces neutron radiation. Although the SF rate is usually negligible when compared with the (α,n) production rates, ^{244}Cm is a notable exception. According to Brookhaven National Laboratory National Nuclear Data Center's NuDat 3.0 tool, the SF yield of ^{244}Cm is 1.4E-4 %, which is almost 1,000 times greater than the ^{228}Pu SF yield (Mason 2021).

The goal of this work is to calculate the radiological dose consequences of each of the eight candidate isotopes under consideration and estimate the radiation shielding required to reduce the dose to safe occupational levels. Each isotope will be examined in the appropriate oxide fuel form in quantities sufficient to generate 100 W_{Th} for 20 years of operation, except for ^{228}Th, which was only considered for 5 years of operation because of its short half-life.

2. ASSUMPTIONS

Key assumptions of this study are listed below.

- Heat generation from the decay products of ^{238}Pu, ^{241}Am and ^{244}Cm is negligible.
- The decay products of ^{90}Sr, ^{227}Ac, ^{228}Ra, ^{228}Th, and ^{232}U are in secular equilibrium.
- Trace contaminants (e.g., production waste products, other isotopes of the same element as the fuel) were neglected for all radioisotopes considered in this study, except for ^{238}Pu.
- All oxides have significantly reduced ^{18}O abundance (approximately 45% of natural) comparable to the amount that would be present in a quality fuel specification to reduce (α,n) reactions, as in flight qualified fuel.
- The electron cut-off was 100 keV. According to Turner's Eq. (6.14), a 100 keV beta in depleted uranium (DU) (Z=92) would only yield 0.5 % of its energy to bremsstrahlung.
- Bremsstrahlung dose from beta decay emissions was included only in the unshielded doses for all isotopes and was not included in the final shielded calculations for all isotopes except for ^{90}Sr because it contributes to less than 8% of the total dose.
- The gamma ray emissions from ^{90}Sr decay product, ^{90}Y, were neglected based on its minute contribution to the unshielded dose spectrum as shown in Figure 8 in Section 3.2.
- Thermal power scaling was based solely on the peak alpha activity for all isotopes (except ^{90}Sr) because alpha decay typically deposits the most energy locally in the fuel.

3. MATERIALS AND METHODS

NASA flight qualified $^{238}PuO_2$ fuel was used as a benchmark for comparison. As such, each candidate radioisotope in the study was modeled as part of an oxide compound. Actinide oxides are also typically more favorable fuel forms because they have traditionally high temperature melting points. The chemical formula for each radioisotope fuel compound and its theoretical density are tabulated in Table 1.

Table 1. Candidate RPS fuel material properties

Isotope	Oxide compound	Density [g/cm^3]	Reference
^{238}Pu	PuO_2	11.5	(M.B.R. Smith 2018)
^{241}Am	Am_2O_3	11.77	(Toxicological Profile for Americium 2012)
^{244}Cm	Cm_2O_3	11.7	(Posey 1973)
^{227}Ac	Ac_2O_3	9.19	(Perry and Phillips 1995)
^{232}U	U_3O_8	8.3	(Perry and Phillips 1995)
^{90}Sr	$SrTiO_3$	5.1	(Villars and Cenzual n.d.)
^{228}Th	ThO_2	9.86	(Perry and Phillips 1995)
^{228}Ra	RaO	7.6	(Bloxam 1913)

3.1 SOURCE ACTIVITY

After determining the material properties and compositions of the radioisotope fuels, the requisite mass ($m_{100W,i}$) of each isotope, i, required to achieve and maintain a minimum 100 W_{Th} energy output (based on total alpha and beta activities) at the end of a 20-year operating life was estimated using Eqs. (1)

and (2), with one exception: ^{228}Th. The estimation for ^{228}Th was based on only a 5-year operating life because of its very short half-life (1.91 years).

$$m_{100\mathrm{W,i}} = \frac{100\ [\mathrm{Watts}]}{P_{\mathrm{s},i} \cdot e^{-(\lambda_i \cdot 20\ [years])}}, \tag{1}$$

where

$$P_{\mathrm{s},i} = \frac{\max\{A_{\mathrm{s},i}(t)\} \cdot 3.7 \times 10^{10}\left[\frac{\mathrm{Bq}}{\mathrm{Ci}}\right] \cdot 1000\left[\frac{\mathrm{eV}}{\mathrm{keV}}\right] \cdot E_{\mathrm{decay}}}{6.2415 \times 10^{18}\left[\frac{\mathrm{eV}}{\mathrm{J}}\right]}, \tag{2}$$

and

$$\overline{E}_{\mathrm{decay}} = \sum_{j=1}^{N-1} \sum_{k=1}^{M} l_{i,j,k} \cdot \overline{E}_{\lambda,i,j,k,}, \tag{3}$$

where

$P_{\mathrm{s},i}$ = the specific power [W/g],
$A_{\mathrm{s},i}$ = the peak specific alpha (or beta for ^{90}Sr) activity [Ci/g] calculated by ORIGEN,
λ_i = the decay constant [s^{-1}],
$l_{i,k}$ = the fractional yield of decay radiation, k,
$\overline{E}_{\lambda,i,k}$ = the mean decay energy [keV] of alpha or beta radiation, k, emitted by decay product, j,
M = the total number of alpha and beta radiation emissions per isotope, i.
N = either a long-lived decay product (relative to the parent isotope) or the stable endpoint of the decay chain.

If the initial fuel isotope has a significantly longer half-life than its first decay product, then this product was assumed to be in secular equilibrium (Turner 2007) with the parent fuel. Subsequent short-lived decay products along the decay chain would also be in secular equilibrium with the parent fuel isotope until again a sufficiently long-lived decay product (either with a greater half-life or within an order of magnitude of the parent's half-life) is eventually reached. The long-lived decay product presents a bottleneck in terms of heat production and a natural cutoff point for radiation contributions to the thermal output of the fuel. Additionally, only major decay contributions (i.e., those with fractional yields exceeding 0.1%) were included.

The peak alpha activities (or beta activity in the case of ^{90}Sr, as shown in Figure 2) from which to base each radioisotope's beginning of operating life were found by calculating the total activity of each isotope across a span of 30 years in one-year increments. The total alpha activity of each isotope, including its decay products, as a function of time is shown in Figure 2.

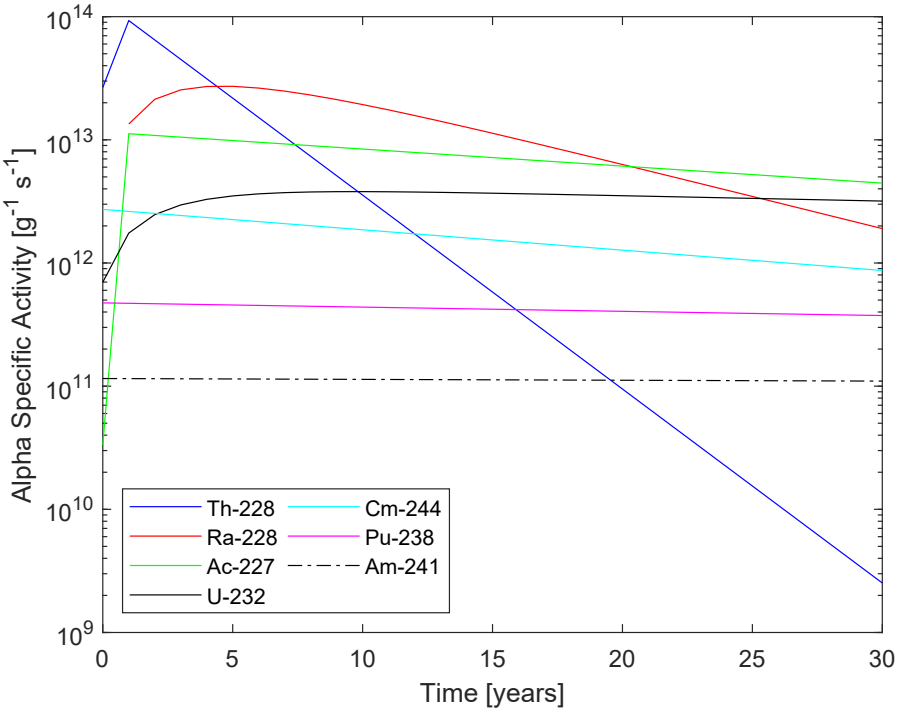

Figure 2. The total alpha particle specific activities of seven candidate RPS fuel materials calculated by ORIGEN over time.

Some isotopes require at least one year of buildup of other alpha producing decay products, such as ^{228}Th, ^{228}Ra, ^{227}Ac, and ^{232}U, whereas the other parent isotopes are the main source of alpha emission which decrease consistently after creation. ^{228}Th and ^{228}Ra have exceptionally high alpha activities and thermal generation potential and are almost two orders of magnitude above the ^{238}Pu baseline. The peak alpha activities computed by SCALE/ORIGEN (Wieselquist et al. 2020), provide the basis for the 100 W_{Th} operating lifetime mass of each oxide fuel as tabulated in Table 2 (along with other important constants). The operating lifetime for all isotopes assumed here is 20 years, except for ^{228}Th, which is only considered for a 5-year operating life as a result of its short half-life.

Table 2. Candidate radioisotope fuel decay data. Unless otherwise noted, peak activities are alpha activities.

Radioisotope Fuel	Half-life [a][a]	Decay constant [a^{-1}]	Mean energy of decay, $\overline{E}_{decay}$ [keV][d]	Peak alpha/beta specific activity [Ci/g]	Minimum initial operating mass ($m_{100W,i}$) [g]	Peak alpha/beta activity [Ci]
$^{238}PuO_2$	87.7	0.007903617	5.487×10^3	12.82	280.9	3,601
$^{241}Am_2O_3$	432.6	0.001602282	5.480×10^3	3.117	1,020	3,179
$^{244}Cm_2O_3$	18.11	0.038274278	5.796×10^3	73.66	84.84	6,249
$^{227}Ac_2O_3$	21.77	0.031839558	3.286×10^4	303.0	3.2	969.6
$^{232}U_3O_8$	68.9	0.010060191	4.090×10^4	102.6	4.9	502.7
$^{90}SrTiO_3$[b]	28.79	0.024075970	1.129×10^3	126.0	191.9	24,180
$^{228}ThO_2$[c]	1.91	0.362904283	3.560×10^4	2,513	1.2	3,016
^{228}RaO	5.75	0.120547336	3.592×10^4	735.2	7.1	5,220

[a] = Half-life data from ENDF VIII.0.
[b] = ^{90}Sr is solely a beta emitter, its peak activities are beta activities.
[c] = ^{228}Th operating half-life is only 5 years, whereas the other isotopes are expected to operate over the course of 20 years.
[d] = Underlying alpha and beta decay energy data are from the Brookhaven National Laboratory NuDat 3.0 tool (Mason 2021).

Although the alpha activity does not directly create an external radiation field concern, other types of radiation produced by each radioisotope and their decay products constitute the basis for occupationally hazardous external radiation fields. These types of radiation include beta (and the secondary bremsstrahlung radiation produced), gamma, and neutron radiations. ORIGEN was also used to calculate beta and gamma activities (Figure 3) and neutron production (Figure 4, including both (α, n) reactions and SF) from each isotope and its decay chain.

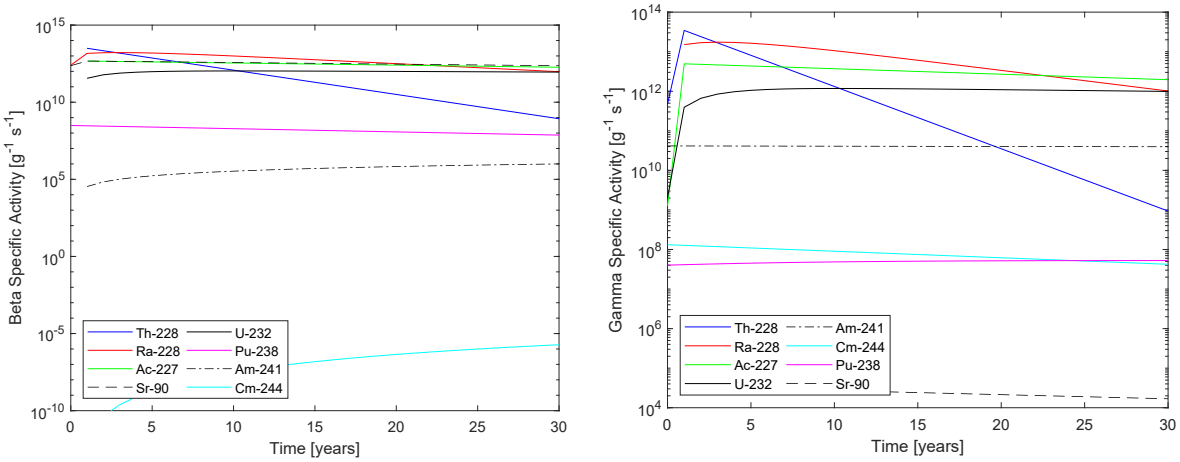

Figure 3. The beta (left) and gamma (right) particle–specific activities of eight candidate RPS fuel materials calculated by ORIGEN as a function of time.

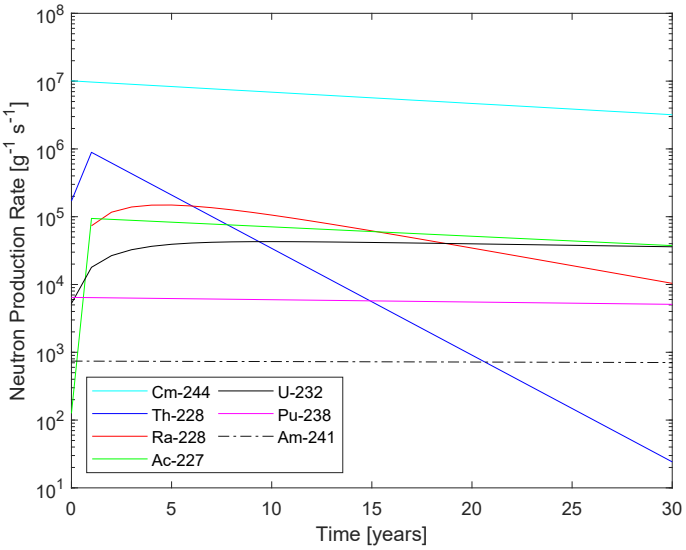

Figure 4. The neutron production rates of seven candidate RPS fuel materials calculated by ORIGEN as a function of time.

The shapes of all three particle activities are fairly similar according to each radioisotope, and they also share the same peak activity year. For example, the peak activity of ^{228}Th can be found at year 1. Hence,

the peak year of beta, gamma, and neutron activity was selected to generate a source term for each radioisotope in all subsequent radiation transport calculations performed using SCALE / Monaco with Automated Variance Reduction using Importance Calculations (MAVRIC). (Peplow 2011) It was assumed that the peak activity would directly correlate to the approximate peak dose fields emitted by each radioisotope.

In reality, the actual dose consequences from the candidate radioisotopes may be higher than predicted by this work. This is because only pure candidate isotope oxide fuels without contaminants were considered (excluding ^{238}Pu). Actual radioisotope fuel is likely to include trace amounts of contaminants, isotopic impurities, and activation byproducts that cannot be removed during radiochemical processing. To gauge the effect of including these trace quantities the differences between pure $^{238}PuO_2$ and flight qualified fuel shown in Figure 5 are considered. Trace quantities within the flight qualified fuel include other isotopes of Pu, especially Pu-236, actinide impurities, and low-Z material impurities. For a complete list of the materials and trace impurities within the "default" RPS-DET fuel composition, please see Figure 29 of the manual. (Michael B. R. Smith et al. 2019)

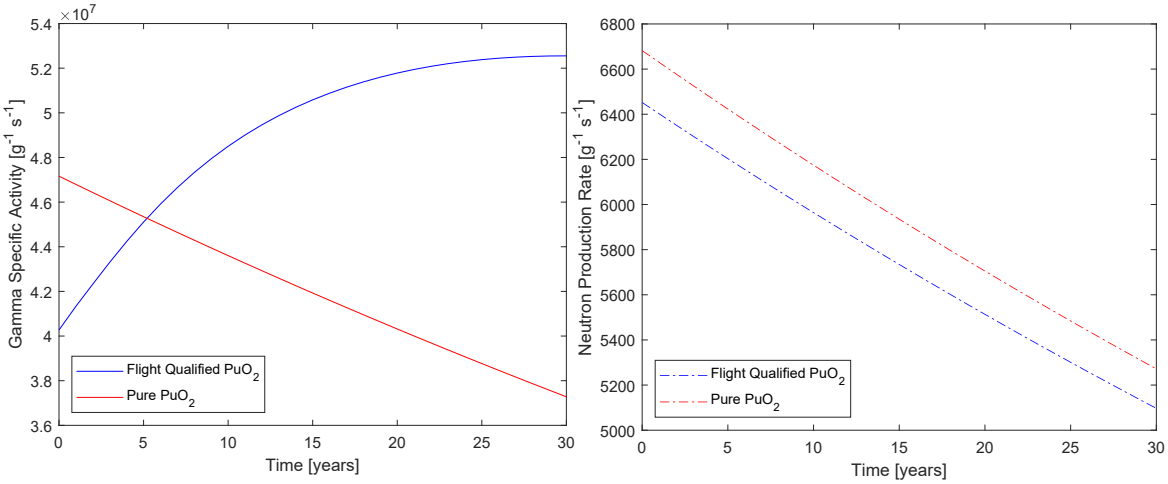

Figure 5. Comparison of the calculated flight qualified PuO_2 fuel (including trace contaminants) gamma (left) and neutron activities to those of pure $^{238}PuO_2$.

The starting magnitudes of the neutron and gamma activities for pure $^{238}PuO_2$ are higher because of the higher concentration of the ^{238}Pu isotope. The neutron activities gradually decrease from creation of both fuels, as expected, because ^{238}Pu is the sole contributor to SF and the main alpha-producing isotope in its decay chain. The majority of neutrons are produced by α,n reactions. Interestingly, the trace contaminants (specifically, Pu-236) within the flight qualified fuel affect the gamma profile much more strongly, gradually building up as the flight qualified fuel decays, quickly overtaking the pure $^{238}PuO_2$ gamma activity. As a result, the peak year of radiation differs greatly between the two fuel types. The peak year of gamma activity for the flight qualified fuel occurs beyond 30 years, with a slow and steady increase, whereas the other peak activities all start at year 0. This is in good agreement with previous RPS – Dose Estimation Tool (DET) benchmarks (M.B.R. Smith 2018). However, because gamma dose is also a function of energy, it is more illustrative to observe the energy-weighted activities shown in Figure 6.

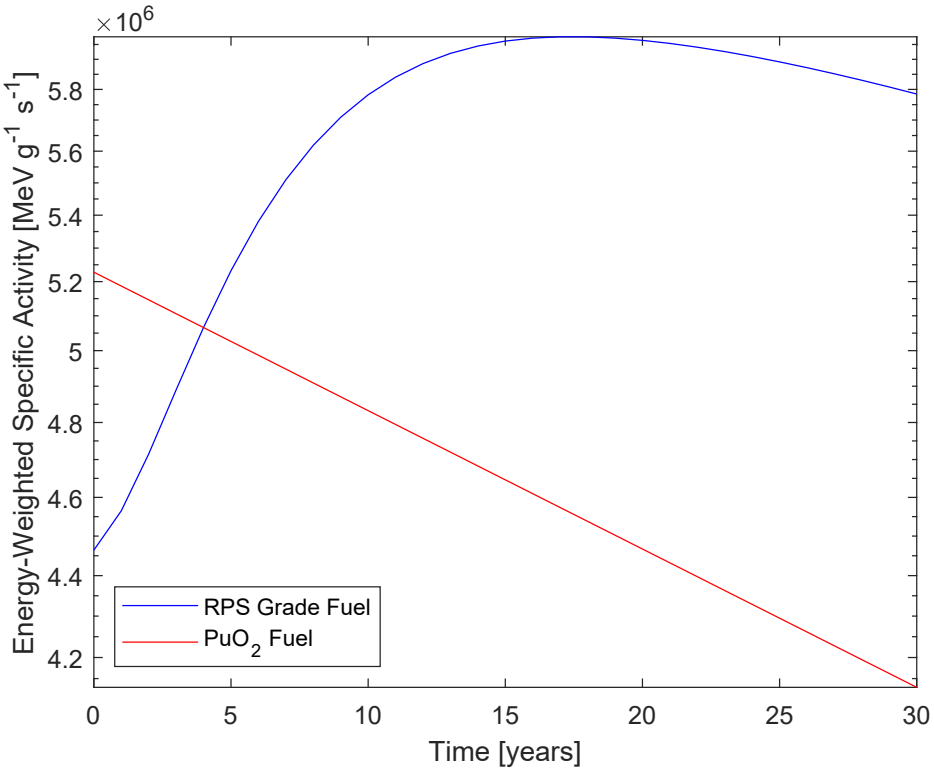

Figure 6. Comparison of the calculated flight qualified PuO_2 fuel (including trace contaminants) energy-weighted gamma activity to those of pure $^{238}PuO_2$.

As expected, the energy-weighted activity is in better agreement with historical observations of peak dose from RPS fuel. The energy-weighted activity peaks at 17 years of age and then declines gradually, whereas the pure ^{238}Pu oxide gamma activity peak remains at year 0 (fresh fuel). Although lower energy components (e.g., x-rays) may still be increasing in intensity from the build-up of other decay products, the high-energy components, which impact dose more substantially, begin to decrease at that point, corresponding to the ^{236}Pu decay chain. This is why the energy-weighted activity is likely a better predictor of the peak dose year for aged flight qualified ^{238}Pu fuel than the unweighted total gamma activity. This metric is not shown for the other candidate radioisotopes because the peaks of the energy-weighted activity distributions as a function of time occur within the same year as the respective total gamma activity peaks.

3.2 MODEL GEOMETRY

The masses and activities required to achieve a minimum operating thermal output of 100 W_{Th} at the end of 20 years were calculated first. For that given quantity of radioisotope, the radiation dose fields and the shielding required to attenuate those fields to reasonable occupational levels were calculated through the Consistent Adjoint Driven Importance Sampling (CADIS)-assisted Monte Carlo radiation transport simulations in SCALE/MAVRIC. The calculated mass and known oxide densities (Table 1) were used to determine the volume of a sphere of oxide fuel for each radioisotope. Next, each fuel sphere was encapsulated by a 1 mm thick Ir cladding, followed by a shell of graphite (to attenuate neutrons) and a shell of DU to attenuate photons. The Ir cladding thickness is based on the 0.8 mm cladding of fueled clads within the RPS-DET. (Michael B. R. Smith et al. 2019) A representative example of the simple MAVRIC geometry that is used for most candidate radioisotope fuel shielding is shown in Figure 7, along with the specialized shielding model developed for the intense neutron radiation field of ^{244}Cm.

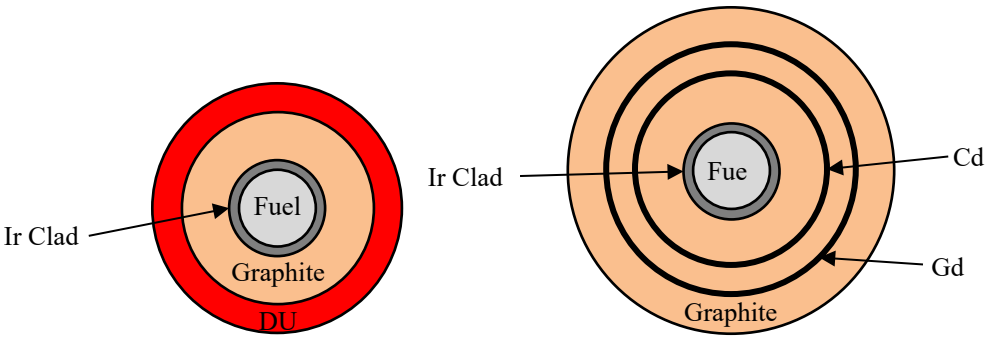

Figure 7. A generalized radiation shielding model (left) for most candidate radioisotope fuel simulations and the specialized shielding developed for ^{244}Cm (right).

The requisite amount of neutron shielding was found by incrementally increasing the graphite thickness until the neutron dose fell below 1 mrem/hr on contact. Once determined, incremental thicknesses of DU shells were added to that of the outside of the graphite shield if necessary to attenuate the gamma or bremsstrahlung radiation field to occupational levels. In a few cases, the gamma radiation field's energy was low enough in intensity that the graphite shielding proved sufficient to attenuate both neutron and gamma radiation. For the MAVRIC models, an approximately 2.3 m × 2.3 m × 1.8 m uniform cartesian mesh with ~10 cm × ~10 cm × 182.44 cm (6 ft.) voxels was implemented with 1977 American National Standards Institute (ANSI) dose response functions to determine the dose on contact and at 30 cm from the source. Such a large mesh was not required for most cases but was kept for simplicity. The voxel sizes were varied in the *x* and *y* dimensions from 9.5 to 10.5 to maintain a consistent location for the on-contact dose tally without changing the outer mesh boundaries.

4. RESULTS

The first set of simulations was designed to determine the unshielded contact dose and the dose at 30 cm away. In reality, the fuel will likely never be truly exposed, because it must be encapsulated (i.e., within the 1 mm Ir cladding) for typical operational scenarios and safety considerations, such as preventing the accidental contamination of the storage containers, personnel, and equipment that will handle the thermoelectric fuel, preventing dissolution of the fuel in water, and particulate release. The bare dose results are displayed in Table 3 and Figure 8.

Table 3. Total bare contact dose and dose at 30 cm away of several radioisotopes of 100 W_{Th} operational mass at the peak year of non-alpha radioactivity

Isotope	Oxide compound	Fuel age at peak activity [years]	Bare contact total dose [rem/hr]	Bare total dose @ 30 cm [rem/hr]
^{238}Pu – Pure	PuO_2	0	5.63×10^{-2}	9.40×10^{-3}
^{241}Am	Am_2O_3	0	6.76×10^{-2}	1.29×10^{-2}
^{228}Pu – Flight Qualified	PuO_2	17	1.02×10^{-1}	1.75×10^{-2}
^{244}Cm	Cm_2O_3	0	2.68×10^{1}	4.30×10^{0}
^{227}Ac	Ac_2O_3	1	4.64×10^{2}	6.49×10^{1}
^{232}U	U_3O_8	10	1.36×10^{3}	1.95×10^{2}
^{90}Sr	$SrTiO_3$	1	1.43×10^{3}	2.67×10^{2}
^{228}Th	ThO_2	1	1.05×10^{4}	1.44×10^{3}
^{228}Ra	RaO	3	3.56×10^{4}	5.15×10^{3}

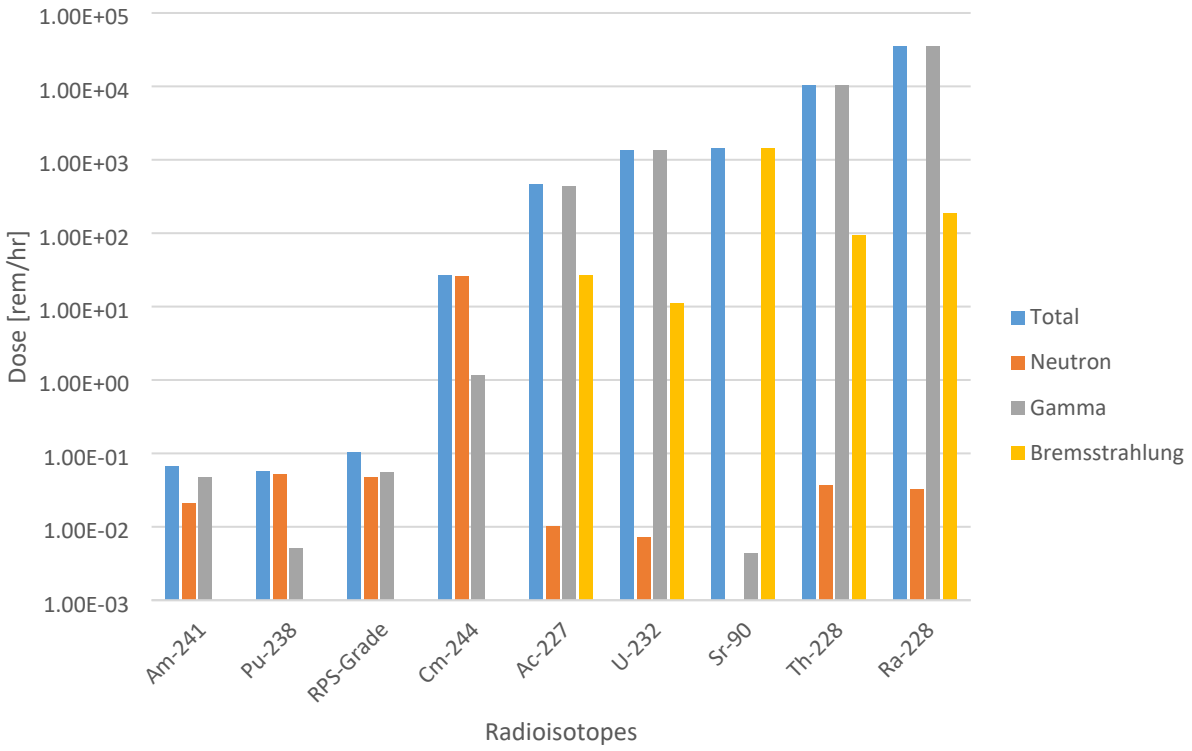

Figure 8. The bare, contact neutron, gamma, bremsstrahlung, and total doses calculated by MAVRIC (i.e., neutron and gamma dose) and Monte Carlo N-Particle (MCNP) (bremsstrahlung) for 100 W_{Th} operating mass spheres of various radioisotopes at their respective ages of peak activity as listed in Table 3.

The table shows the peak activity years selected. As shown in Figure 3 and Figure 4, the peak activity for most of the candidate radioisotopes occurs within the first 5 years after production. The two exceptions are ^{232}U and ^{238}Pu (flight qualified fuel), which have the two longest buildup periods for gamma-emitting decay products. In both cases, this is the buildup of a decay product, ^{208}Tl, which is common to both radioisotope fuels. ^{236}Pu is a common impurity from the production of flight qualified fuel, and ^{232}U is part of the ^{236}Pu decay chain, thus producing ^{208}Tl. ^{208}Tl is a high-activity source of 2.6 MeV gamma rays, and it is the main contributor to a gamma dose of flight qualified fuel that is nearly doubled over pure $^{238}PuO_2$ fuel.

The reason that the dose from flight qualified fuel was compared to that from pure $^{238}PuO_2$ fuel was to estimate the potential impact of trace contaminants and isotopic impurities, which were neglected in the other radioisotope fuels. All subsequent calculations included flight qualified fuel only for comparison with historical results. Therefore, any subsequent references to ^{238}Pu refer to flight qualified fuel (starting in Figure 8 above). Clearly, the additional radiation emitted from isotopic impurities can be significant, so all dose values and shielding thicknesses (with the exception of ^{238}Pu) shown within this work should be considered ideal minimums.

Figure 8 provides a more in-depth analysis of the candidate radioisotopes and the individual radiation types (excluding alpha) that are significant to the total dose. The radioisotopes are organized from lowest to highest total dose. The bremsstrahlung hazard from ^{90}Sr is well known historically (Shor et al. 1971). Note that there is also a very small 2.186 MeV gamma ray contribution (< 1E-3 % of the total dose) from ^{90}Y, a decay product of ^{90}Sr, which is negligible. Any high-Z shielding provided to attenuate

bremsstrahlung will also function effectively for primary gamma rays. The converse is true for the isotopes with gamma ray doses that are much higher than bremsstrahlung. Most of the candidate isotopes produce significant gamma radiation (>90% of the total dose) with the exception of the three with the lowest total doses (first three from the left). The bare neutron doses are fairly comparable among the considered radioisotopes (with the exception of ^{244}Cm). This is because the quantities of each radioisotope fuel are scaled to the same thermal output based on alpha activity, and neutron production is largely governed by (α, n) reactions. However, ^{244}Cm has an exceptionally high neutron dose, nearly 1,000 times greater than the other isotopes. This is mainly because of its naturally high SF rate.

To provide better context to how significant the unshielded dose is from the majority of the candidate radioisotope fuels, Figure 9 compares the total contact dose rate per minute of exposure to each of the radioisotope heat sources to the lethal dose levels (Craig and Jungerman 1990) and the US occupational dose annual limit (10 CFR 835.202 Occupational dose limits for general employees 2007) as a lower bound.

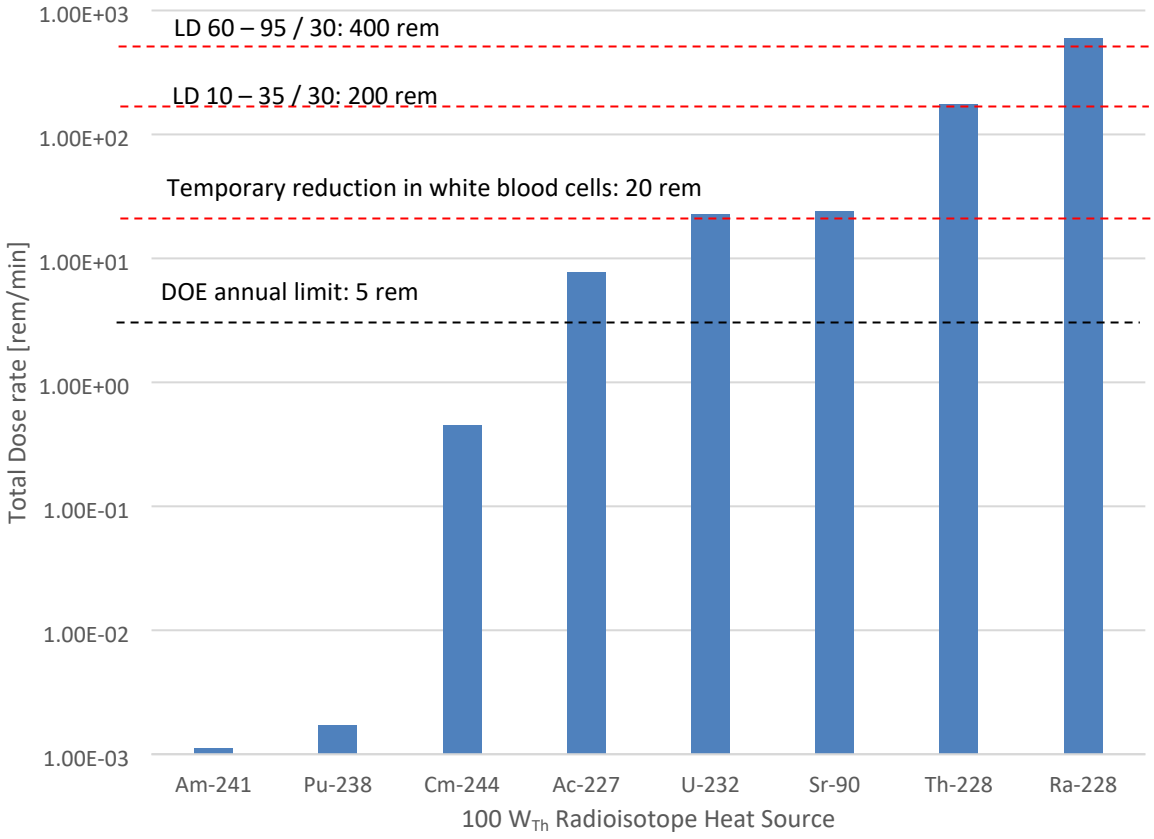

Figure 9. The calculated peak unshielded total contact dose rates (rem/min) for each of the radioisotope heat sources, which are normalized to a 100 W_{Th} operating mass and compared to acute dose thresholds and the DOE annual occupational limit.

Within one minute of exposure, all the candidate radioisotope fuels shown to the right of ^{244}Cm exceeded the DOE annual limit, and ^{244}Cm would easily exceed that limit within six minutes. Those to the right of ^{227}Ac will quickly induce acute radiation effects within personnel exposed to the radioisotopes. Ra-228 even exceeds the LD 60-95/30 dose limit – the lethal dose at which 60-95% of an exposed population

would be expected to die within 30 days. Consequently, it is highly recommended that all sources shown to the right of ^{238}Pu be handled remotely by robotic equipment when bare or essentially unshielded. Operators should employ radiation shielding at all times to handle these sources safely. It is typical even for traditional flight qualified PuO_2 fuel to be handled in either shielded gloveboxes or hot cells (depending on the amount of fuel present).

To properly shield the radiation fields emitted by the eight radioisotope fuel spheres to occupational levels, a neutron radiation shield (graphite) was added as an outer shell, (as depicted in Figure 7). Then, if necessary, a secondary gamma radiation shield (composed of depleted uranium) was added as a second shell. Figure 10 displays the calculated neutron dose as a function of the increasing thickness of graphite.

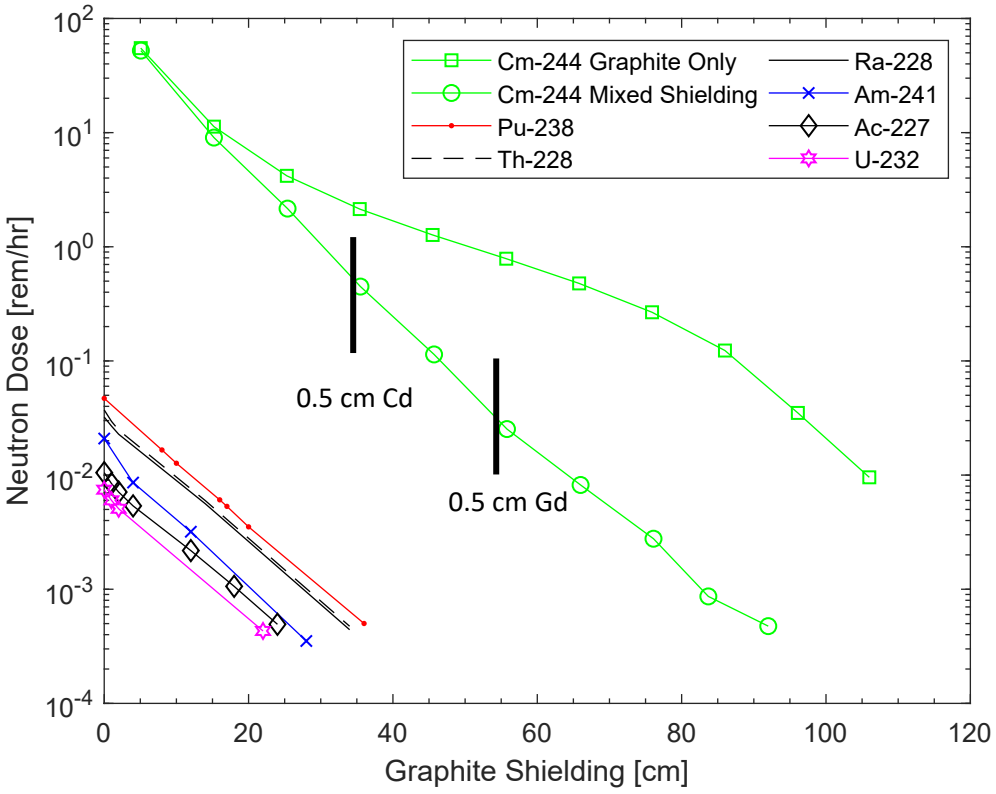

Figure 10. The calculated on-contact neutron dose of several radioisotopes as a function of graphite shielding thickness (or mixed shielding, only in the case of ^{244}Cm).

As expected, the radioisotope magnitudes are proportional to the calculated neutron dose (with ^{244}Cm being the highest, followed by ^{238}Pu). For most of the candidate radioisotopes, the neutron dose on contact was already under 100 mrem/h and can easily be decreased to less than 1 mrem/h with 35 cm of graphite or less. The majority of the radioisotope dose curves (except for that of ^{244}Cm) also present a fairly decreasing exponential pattern (linear in appearance on a logarithmic scale), as is typical of neutron attenuation. ^{244}Cm was the only exception, having required the addition of thin layers of Cd and Gd metal shielding (0.5 cm) between shells of graphite (shown in Figure 7) to maintain efficient exponential attenuation of neutrons throughout the graphite shield. Without attenuation, the neutron dose flattens off significantly after 30 cm of shielding because graphite is a better moderator than absorber.

Because of the complex nature of the mixed shielding and the overall large amount of shielding required, the ^{244}Cm shielding calculation was performed upon a contiguous mesh, whereas the other radioisotope shielding calculations were performed individually, with incrementally increasing shielding. Any calculated dose value shown to the left of the ^{244}Cm endpoint (which was on contact, outside of the shield), is within the shield. Such values tend to underestimate the actual dose value by providing several extra centimeters of attenuation across the length of the mesh cell.

Three radioisotopes studied in this work—^{244}Cm, ^{238}Pu, and ^{241}Am—emitted relatively low intensity gamma radiation fields and did not require additional shielding beyond that of the graphite already employed for neutron shielding. The photon dose as a function of graphite thickness for these three isotopes can be seen in Figure 11.

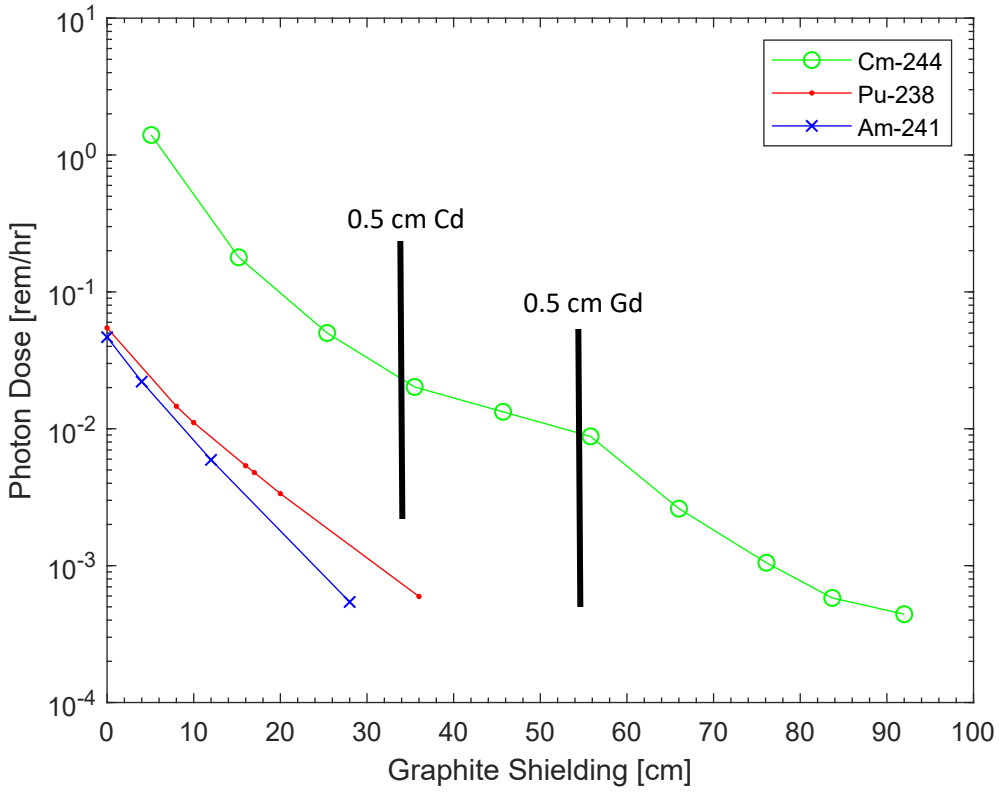

Figure 11. The calculated on-contact photon dose as a function of graphite shielding thickness for several isotopes. ^{244}Cm includes two additional 0.5 cm shells (one of Cd and another of Gd metal) inserted between graphite shells at radial distances of 35 and 55 cm, respectively.

The photon dose profile exhibits a similar exponential attenuation behavior (linear on a logarithmic scale) similar to the neutron dose profile. Even the dose profile of the contiguous ^{244}Cm mixed shield is relatively linear away from material transition boundaries. The photon dose falls under 1 mrem/h for ^{241}Am and ^{238}Pu within approximately 35 cm of graphite shielding, whereas ^{244}Cm requires approximately 90 cm of mixed shielding to accomplish the same reduction in dose.

The other five candidate radioisotope fuels require additional gamma shielding. In this work, that was accomplished by incrementally adding DU shells around the inner shell of graphite shielding—or mixed

shielding in the case of ^{244}Cm (of the endpoint thicknesses shown in Figure 10). The resulting photon dose profiles as a function of additional DU shielding thickness are shown in Figure 12.

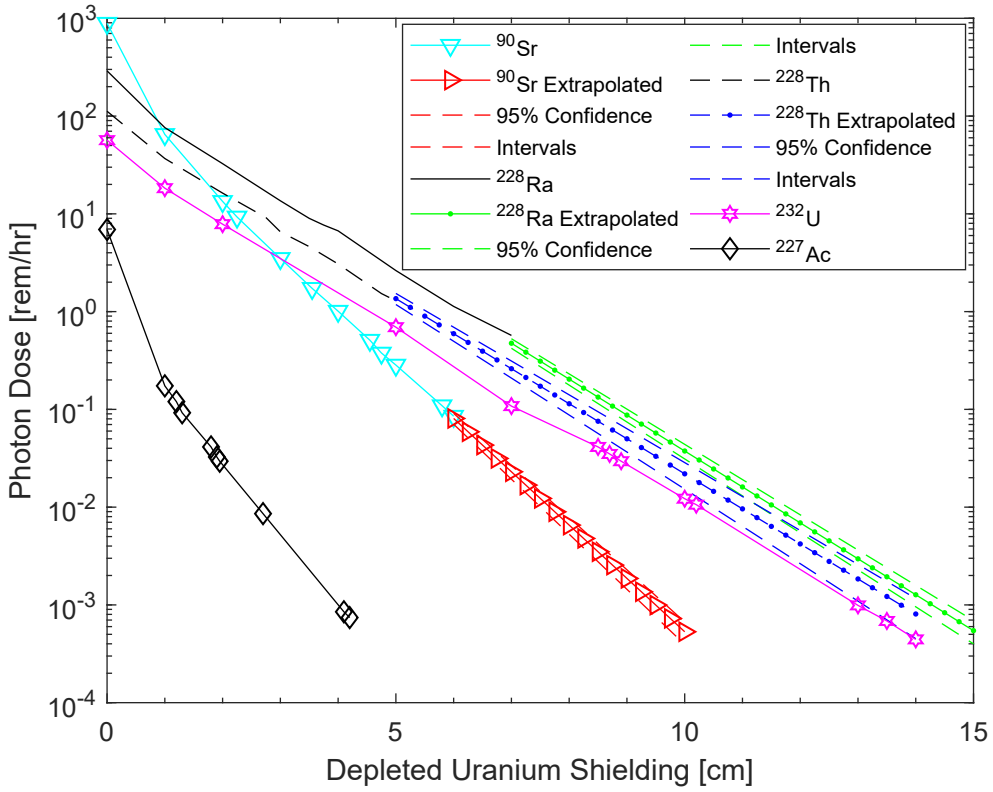

Figure 12. The calculated on-contact photon dose as a function of an outer shell of DU shielding thickness overlaying the prior inner shell of graphite (shown in Fig. 10) of a thickness equal to the amount of the shielding required alone to reduce the on-contact neutron dose to approximately 5×10^{-4} rem/h.

As expected, the magnitudes of the radioisotope photon dose profiles are proportional to the activities predicted by ORIGEN, and the profiles follow an exponential decreasing behavior beyond the 1 cm. The steeper curve between 0 and 1 cm of DU shielding is likely an artifact of the material transition boundary between the inner graphite and outer DU shells. Detailed dose values per thickness are tabulated in Table A-1 in the Appendix. This traditional exponential behavior is important to note because it allows the reasonable extrapolation of photon doses according to half and tenth value thickness (TVL) principles (Shultis and Faw 2000).

Accordingly, a simple first-order exponential nonlinear least-squares curve fit was performed. The fit parameters and goodness-of-fit statistics are listed in Table 4, and the relative residuals are shown in Figure 13.

Table 4. Fit parameters for the exponential ($f(x) = ae^{bx}$) curve fits of the extrapolated photon doses in Figure 10

Isotope	a	b	χ^2_{red}	Max. relative residual
^{90}Sr	151.3	-1.256	10.027	0.0841
^{228}Ra	177.5	-0.8462	1.7008	0.1683

^{228}Th	84.13	-0.8253	2.4854	0.0909

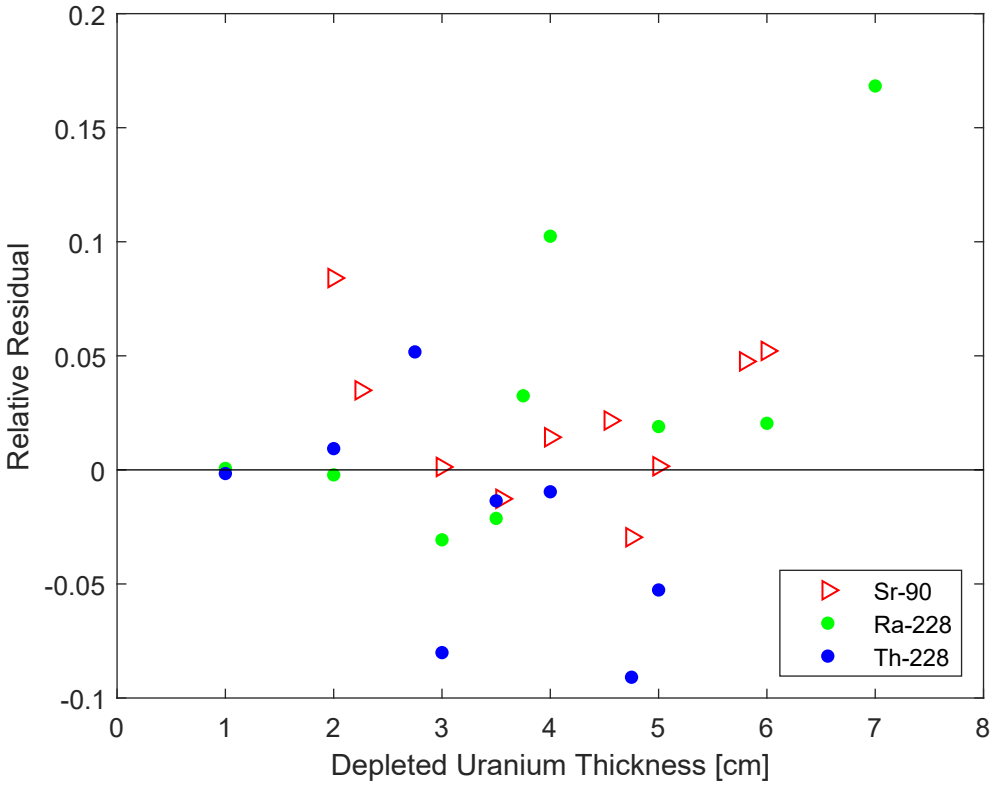

Figure 13. The relative residuals differences between the SCALE/MAVRIC calculated dose and the exponential fit predictions for each radioisotope as a function of DU thickness.

The reduced χ^2 test (R. C. Smith 2014) for ^{90}Sr is close to 10 and acceptable. The χ^2_{red} values for ^{228}Ra and ^{228}Th are closer to the ideal value of 1. The relative residuals (R_{rel}) shown in Fig. 13 are of the form:

$$R_{\text{rel}} = \frac{D_c - D_{\text{fit}}}{D_c}, \tag{4}$$

where D_c is the calculated dose and D_{fit} is the dose predicted by the exponential fit. ^{90}Sr and ^{228}Ra have a higher number of positive residuals, so the extrapolated dose could slightly underpredict the amount of gamma radiation shielding required to reduce the dose to occupational levels. Whereas the ^{228}Th residuals are primarily negative, so the amount of shielding could slightly be overpredicted. There are no apparent patterns or evidence of bias in any of the three sets of radioisotope residuals, and therefore, it is unlikely that the selection of a higher order fit model or a more rigorous tuning of the fit parameters would produce significant improvements. Please note, however, that a more robust curve fitting method known as *bisquare weights* was used on ^{90}Sr to ensure lower residuals at a slight cost (or increase) to the χ^2_{red} value.

To summarize, ^{90}Sr, ^{232}U, ^{228}Th, and ^{228}Ra all require substantial gamma (or bremsstrahlung) radiation shielding to reduce their dose fields to acceptable occupational levels, and ^{244}Cm requires substantial

neutron shielding. Whereas, ^{238}Pu and ^{241}Am require only nominal shielding. Detailed dose thresholds and shielding thicknesses required to reach them are shown in Table 5.

Table 5. Specific shielding thicknesses [cm] required to reach several contact dose thresholds

Isotope	Inner graphite shielding	DU shielding thickness required to reach 100 mrem/h	DU shielding thickness required to reach 30 mrem/h	DU shielding thickness required to reach 10 mrem/h	DU shielding thickness required to reach 1 mrem/h
^{238}Pu[a]	N/A	0.0	8.0	17.0	36.0
^{241}Am[a]	N/A	0.0	4.0	12.0	28.0
^{90}Sr	N/A	5.8	**6.8**	**7.7**	**9.5**
^{244}Cm[b]	Special	48.7	57.6	67.1	85.0
^{227}Ac	24	1.3	1.9	2.7	4.2
^{232}U	22	7.0	8.9	10.2	13.0
^{228}Th	34	**8.2**	**9.7**	**11.0**	**14.0**
^{228}Ra	34	**8.9**	**10.3**	**11.6**	**14.3**

[a] = Only a single shield of graphite is needed to attenuate these isotopes.
[b] = Because of the complex nature of ^{244}Cm's mixed neutron shielding, these values are not on-contact doses but are interpolated estimates from a mesh overlaying the entire shield. Actual dose shielding may be slightly higher.
Note: bold values represent mean shielding prediction values from curve fit estimations.

0.1 rem/hr (100 mrem/hr) and 10 mrem/hr on-contact dose thresholds were selected to approximately bound the need for considering the area immediately surrounding a candidate radioisotope heat source as a high radiation area vs. a radiation area (according to 10 CFR 20.1003). The other thresholds were selected merely for tracking trends.

As a consequence of the thick shielding for six of the eight 100 W_{Th} RPS fuels considered, the masses and volumes required could be prohibitive for space applications. That ordering was not selected to minimize mass and volume of the shield. The original ordering of the configuration was selected to simply minimize potential dose consequences arising from (n, γ) effects. However, those effects may also be mitigated with additional lightweight shielding if necessary, although the gamma shield may not absorb enough neutrons to create a significant (n, γ) dose contribution. Reversing the order of the shielding may lower the total mass and volume of the shield by placing the heaviest materials closer to the source. An in-depth analysis of materials and geometries for optimizing the weight of mixed shielding is beyond the scope of this study. However, a better estimate of the lower bound of shielding weight can still be obtained by observing the total dose attenuation curves corresponding to a pure DU shield. Additionally, the gamma source contribution from the five highest candidate radioisotope fuels is nearly five orders of magnitude higher than the neutron dose (Figure 8), so even a poor neutron shield such as DU may be sufficient alone to mitigate the total dose from both particle types. Figure 14 and Figure 15 show the effects of a pure DU shield on gamma and photon dose, respectively, for ^{232}U, ^{228}Th, ^{228}Ra, and ^{227}Ac.

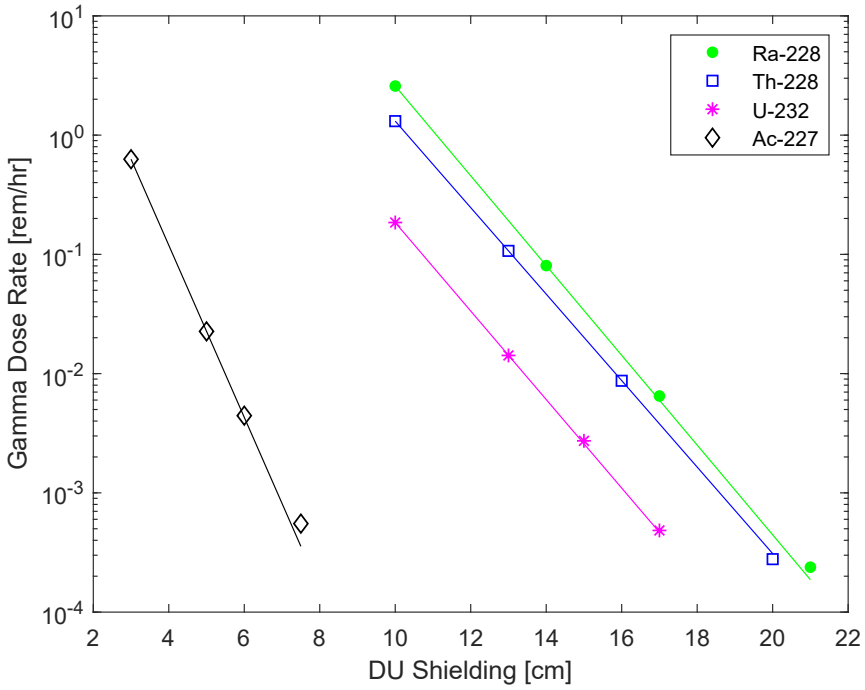

Figure 14. The SCALE-calculated photon dose as a function of DU shielding thickness and the corresponding exponential curve fits (i.e., continuous lines) for TVL-based interpolation.

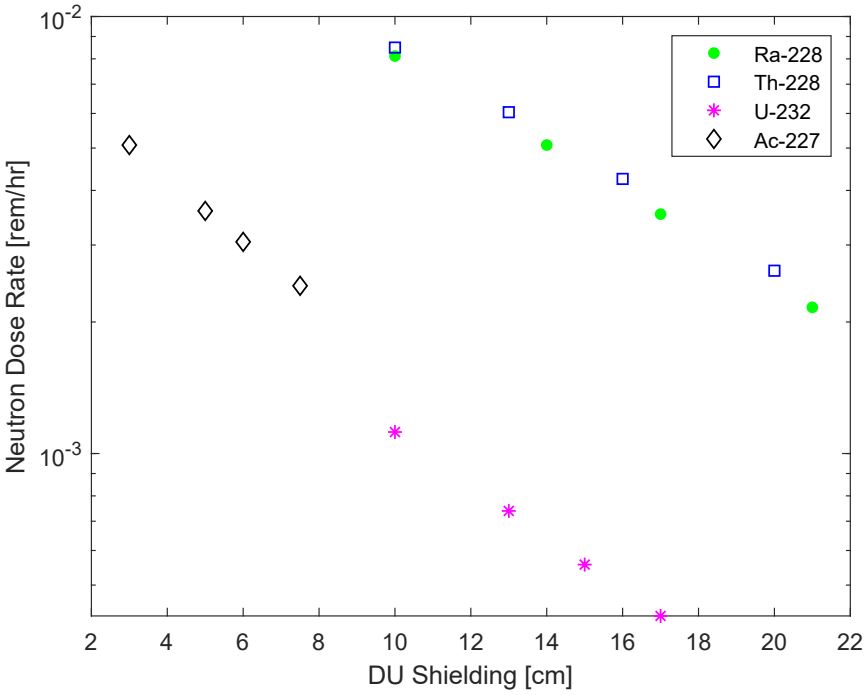

Figure 15. The SCALE-calculated neutron dose as a function of DU shielding thickness.

Initial shielding thicknesses were selected based on the required number of TVLs (estimated from the previous two shell shielding calculations in Fig. 12) to lower the gamma dose to approximately 1 rem/hr, which were 10 cm for ^{228}Ra, ^{228}Th, and ^{232}U and 3 cm for ^{227}Ac. On average, a pure DU shield required 2–7 cm of additional material to reduce the gamma dose to similar values seen in the mixed shielding calculation (Figure 12 and Figure 13). As expected, the DU shield still reduced the neutron dose to some degree by acting as a spacer for geometric attenuation, at a minimum. The decrease is slightly less than the ideal square law predictions because the source is still too close to the outer surface of the shield to be fully approximated as a point source. Overall, the neutron dose is negligible for ^{232}U and is also negligible for the other three isotopes until the gamma dose is dampened below 1 mrem/h. Additional shielding will be necessary to reduce the neutron dose below 1 mrem/h for ^{228}Th, ^{228}Ra, and ^{227}Ac.

Even though DU shielding appears to be mostly sufficient by itself, it is also worth comparing the total mass and volume of both DU-only and mixed shielding configurations for several dose thresholds. The volume and mass as a function of total dose are shown for all three shielding configurations (mixed, pure DU, and pure graphite) in Figure 16 and tabulated in Appendix Table 1 as well.

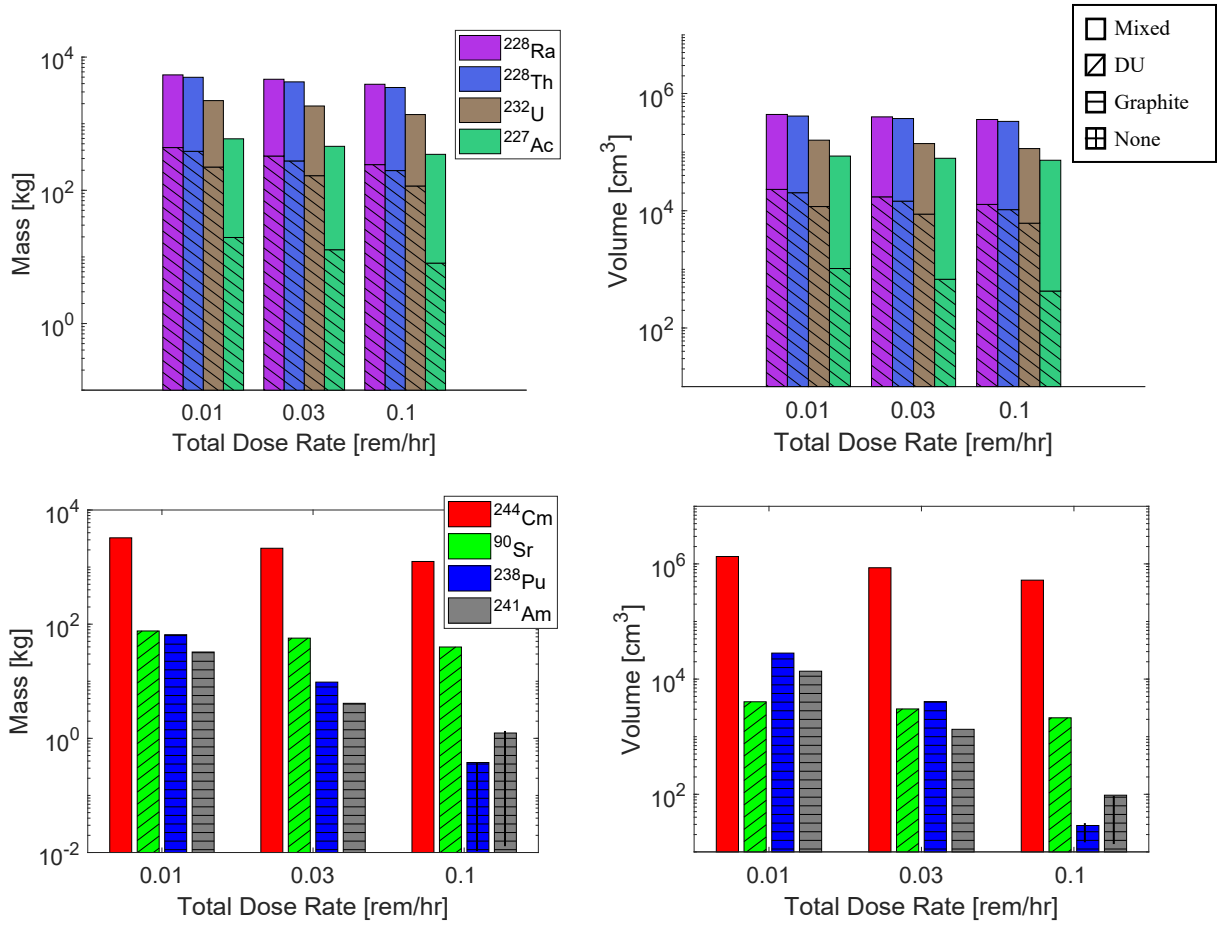

Figure 16. Comparison of the total mass (upper left) and volume (upper right) of the mixed and pure DU shielding configurations of ^{227}Ac, ^{232}U, ^{228}Th, and ^{228}Ra as a function of total dose rate (0.1, 0.03, and 0.01 rem/hr) and a similar comparison of the mass (lower left) and volume (lower right) of the other isotopes.

As predicted, switching to a pure DU shield substantially lowers the mass required to shield ^{227}Ac, ^{232}U, ^{228}Th, and ^{228}Ra from 100 – 1,000 of kg to 10 –100s of kg, and similarly, it lowers the volume by over an

order of magnitude. The pure DU-shielded gamma doses were exponentially interpolated (as seen in Figure 15), and the neutron doses were linearly interpolated for the first four isotopes as necessary. (n, γ) contributions to the gamma dose were calculated and negligible. Doses below 10 mrem/h were not considered for pure DU shielding of the four isotopes because three of the four would require additional neutron shielding, as seen in Figure 14 and Figure 15. For ^{227}Ac, ^{228}Th, and ^{228}Ra at 10 mrem/h, the neutron dose of each is ~3 mrem/h (or ~⅓ of the total dose), so the neutron dose begins to overtake the gamma dose. Please note that in the 0.1 rem/hr case, ^{238}Pu and ^{241}Am required no shielding and the mass shown is purely that of the fuel and cladding alone.

5. CONCLUSION

This work compares the radiation dose consequences of seven candidate radioisotope thermoelectric fuels to the current US baseline RPS fuel, $^{238}PuO_2$. All fuels were examined in oxide form, of quantities sufficient to provide 100 W_{Th} of power for a 20-year (5-year for ^{228}Th) operating lifetime, and at the age of peak radiation emissions.

Although ^{227}Ac, ^{232}U, ^{90}Sr, ^{228}Th, and ^{228}Ra have the highest thermal outputs (based on alpha activity or beta in the case of ^{90}Sr), they emit dangerous photon radiation fields when bare. These isotopes will likely require significant radiological mitigation if manufactured into RPS fuel, even for small quantities. Of the five isotopes, ^{227}Ac requires the least amount of shielding at 4.13 cm of DU to reduce the total dose rates to 100 mrem/h on contact, with ^{90}Sr being the next lowest at 5.8 cm. For perspective, the total weight of one 100 W_{Th}, ^{227}Ac radioisotope heat source equates to 8 kg of mass, including the fuel and cladding. A few small tradeoffs with lower density, higher volume shields could be implemented to slightly reduce the mass requirements, but significant reductions should not be expected. Additionally, scaling up to the approximate MMRTG equivalent thermal power output of 2 kW (Lee and Bairstow 2015), would multiply this weight by approximately a factor of 20, resulting in a total of ~160 kg (nearly three times the MMRTG's total weight) of shielding at a minimum. Therefore, it may be challenging to implement these into a lightweight RPS.

^{244}Cm would also likely require significant radiological mitigation because of its intense on-contact neutron dose rate. Furthermore, it requires the most substantial shielding overall, with nearly 49 cm of graphite required to reduce the total dose rate to 100 mrem/h (which equates to nearly 1.25 Mg of graphite). ^{244}Cm would only make sense for applications where mass and volume are not highly constrained and perhaps would serve better as a neutron source than a thermal source. ^{241}Am and ^{238}Pu continue to be very favorable radioisotopes, requiring the least amount of total shielding overall.

6. REFERENCES

"10 CFR 835.202 Occupational Dose Limits for General Employees." 2007. https://www.ecfr.gov/current/title-10/chapter-III/part-835/subpart-C/section-835.202.

Ambrosi, Richard M. et al. 2019. "European Radioisotope Thermoelectric Generators (RTGs) and Radioisotope Heater Units (RHUs) for Space Science and Exploration." *Space Science Reviews* 215(55): 41.

American Nuclear Society. 2021. "DOE Steps up Plutonium Production for Future Space Exploration." *Nuclear Newswire: Research & Applications*. https://www.ans.org/news/article-2658/doe-steps-up-plutonium-production-for-future-space-exploration/ (September 1, 2022).

Anderson, G. M., and F. H. Featherston. 1960. "The SNAP Programme. US AEC's Space-Electric Power Programme." *Nuclear Engineering* 5.

Bennett, Gary L., Richard J. Hemler, and Alfred Schock. 1996. "Status Report on the U.S. Space Nuclear Program." *Acta Astronautica* 38(4–8): 551–60.

Bloxam, Charles Loudon. 1913. *Chemistry, Inorganic and Organic: With Experiments*. 10th ed. Philadelphia: P. Blakiston's Son & Co. https://books.google.com/books?id=vIQ-AAAAYAAJ&pg=PA307&lpg=PA307&dq=Radium+Oxide+density&source=bl&ots=PDVmQSFHJs&sig=ACfU3U2vJHOUA81D7iRFdKUHXEYO5gsEHw&hl=en&sa=X&ved=2ahUKEwiQt-D93dj4AhXbEGIAHcJzDaQ4ChDoAXoECBcQAw#v=onepage&q=Radium%20Oxide%20density&f=false.

Craig, Paul P., and John A. Jungerman. 1990. *The Nuclear Arms Race: Technology and Society*. 2nd ed. McGraw-Hill College.

Dustin, J. Seth, and R. A. Borrelli. 2021. "Assessment of Alternative Radionuclides for Use in a Radioisotope Thermoelectric Generator." *Nuclear Engineering and Design* 385(111475): 13.

"JANIS." 2013. https://www.oecd-nea.org/janis.

Lee, Young, and Bryan Bairstow. 2015. *Radioisotope Power Systems Reference Book for Mission Designers and Planners*. Pasadena, CA: NASA Jet Propulsion Laboratory.

Mason, Donnie. 2021. "NuDat." https://www.nndc.bnl.gov/nudat3/.

Peplow, Douglas E. 2011. "Monte Carlo Shielding Analysis Capabilities With Mavric." *Nuclear Technology* 174: 289–313.

Perry, Dale L., and Sidney L. Phillips. 1995. *Handbook of Inorganic Compounds*. Boca Raton, FL: CRC Press. https://books.google.com/books?id=0fT4wfhF1AsC&pg=RA1-PA2&lpg=RA1-PA2&dq=density+of+ac2o3&source=bl&ots=EERO0-yH3r&sig=ACfU3U35E2GvG2aeeds0F0sDpIhxjW4MVg&hl=en&sa=X&ved=2ahUKEwiNxvalsbD3AhVomXIEHYJ2CucQ6AF6BAgeEAM#v=onepage&q=density%20of%20ac2o3&f=false (September 1, 2022).

Posey, J. C. 1973. "Curium-244 Isotopic Power Fuel - Chemical Recovery from Commercial Power Reactor Fuels." In Detroit, MI: AIChE, 1–33. https://www.osti.gov/biblio/4485122.

Shor, Roberta, Robert H. Jr. Lafferty, and P. S. Baker. 1971. *Strontium-90 Heat Sources*. Oak Ridge, TN: Oak Ridge National Laboratory.

Shultis, J. K., and Richard E. Faw. 2000. *Radiation Shielding*. La Grange Park, IL: American Nuclear Society.

Smith, M. B. R. 2018. “Radioisotope Power System Dose Estimation Tool (RPS-DET).” In Big Sky, MT: IEEE, 19.

Smith, Michael B. R., Douglas E. Peplow, Robert A. Lefebvre, and William Wieselquist. 2019. *Radioisotope Power System Dose Estimation Tool (RPS-DET) User Manual*. Oak Ridge National Laboratory. https://doi.org/10.2172/1560442.

Smith, Ralph C. 2014. *Uncertainty Quantification: Theory, Implementation, and Applications*. Illustrated. Philadelphia: Society for Industrial and Applied Mathematics.

Toxicological Profile for Americium. 2012. Chamblee, GA: Agency for Toxic Substances and Disease Registry. https://www.atsdr.cdc.gov/toxprofiles/tp156-c4.pdf (September 1, 2022).

Turner, James. 2007. *Atoms, Radiation, and Radiation Protection*. Third. Weinheim, Germany: Wiley-VCH.

Villars, Pierre, and Karin Cenzual. “SrTiO3 Crystal Structure: Datasheet from ‘PAULING FILE Multinaries Edition – 2012’ in SpringerMaterials.” https://materials.springer.com/isp/crystallographic/docs/sd_0554610.

Wieselquist, W. A., R. A. Lefebvre, and M. A. Jessee. 2020. *SCALE Code System*. Oak Ridge, TN: Oak Ridge National Laboratory. Manual.

APPENDIX A. ADDITIONAL SHIELDING DATA

Table A-1. The mass and volume of various types of shields required to reach several contact dose thresholds.

Isotope	Shield Type	Dose Threshold [mrem/hr]	Mass [kg]	Volume [cm^3]
^{238}Pu	Graphite	100	3.77×10^{-1}	2.87×10^{1}
		30	9.66×10^{0}	4.06×10^{3}
		10	6.54×10^{1}	2.83×10^{4}
^{241}Am	Graphite	100	1.24×10^{0}	9.65×10^{1}
		30	4.11×10^{0}	1.34×10^{3}
		10	3.25×10^{1}	1.37×10^{4}
^{90}Sr	DU	100	3.98×10^{1}	2.13×10^{3}
		30	5.70×10^{1}	3.03×10^{3}
		10	7.60×10^{1}	4.04×10^{3}
^{244}Cm	Mixed, Special	100	1.25×10^{3}	5.22×10^{5}
		30	2.14×10^{3}	8.57×10^{5}
		10	3.25×10^{3}	1.34×10^{6}
^{227}Ac	Mixed	100	3.39×10^{2}	7.22×10^{4}
		30	4.45×10^{2}	7.78×10^{4}
		10	5.74×10^{2}	8.46×10^{4}
	DU	100	8.07×10^{0}	4.26×10^{2}
		30	1.28×10^{1}	6.77×10^{2}
		10	1.96×10^{1}	1.03×10^{3}
^{232}U	Mixed	100	1.26×10^{3}	1.08×10^{5}
		30	1.68×10^{3}	1.31×10^{5}
		10	2.00×10^{3}	1.48×10^{5}
	DU	100	1.16×10^{2}	6.13×10^{3}
		30	1.66×10^{2}	8.75×10^{3}
		10	2.23×10^{2}	1.18×10^{4}
^{228}Th	Mixed	100	3.30×10^{3}	3.24×10^{5}
		30	3.97×10^{3}	3.59×10^{5}
		10	4.59×10^{3}	3.92×10^{5}
	DU	100	1.98×10^{2}	1.04×10^{4}
		30	2.76×10^{2}	1.46×10^{4}
		10	3.85×10^{2}	2.03×10^{4}
^{228}Ra	Mixed	100	3.67×10^{3}	3.47×10^{5}
		30	4.32×10^{3}	3.82×10^{5}
		10	4.97×10^{3}	4.16×10^{5}
	DU	100	2.43×10^{2}	1.28×10^{4}
		30	3.27×10^{2}	1.73×10^{4}
		10	4.38×10^{2}	2.31×10^{4}